

The adsorption and reaction of a titanate coupling reagent on the surfaces of different nanoparticles in supercritical CO₂

Zhi-Wen Wang, Ting-Jie Wang*, Zhan-Wen Wang, Yong Jin

Beijing Key Laboratory of Green Chemical Reaction Engineering and Technology, Department of Chemical Engineering, Tsinghua University, Beijing 100084, China

Received 18 June 2006; accepted 22 August 2006

Available online 26 September 2006

Abstract

The adsorption and reaction in supercritical CO₂ of the titanate coupling reagent NDZ-201 on the surfaces of seven metal oxide particles, SiO₂, Al₂O₃, ZrO₂, TiO₂ (anatase), TiO₂ (rutile), Fe₂O₃, and Fe₃O₄, was investigated. FTIR and TG analysis indicated that the adsorption and reaction were different on different particle surfaces. On SiO₂ and Al₂O₃ particles, there was a chemical reaction of the titanate coupling reagent on the surfaces. On the surfaces of ZrO₂ and TiO₂ (anatase) particles, there were two kinds of adsorption, weak and strong adsorption. On the surfaces of TiO₂ (rutile), Fe₂O₃, and Fe₃O₄ particles, there was only weak adsorption. The acidity or basicity of the OH groups on the particle surface was the key factor that determined if a surface reaction occurred. When the OH groups were acidic, the titanate coupling reagent reacted with these, but otherwise, there was no reaction. The surface density of OH groups on the original particles and the amount of titanate coupling reagent adsorbed and reacted were estimated from TG analysis. The reactivity of the surface OH groups of Al₂O₃ particles was higher than that of the SiO₂ particles.

© 2006 Elsevier Inc. All rights reserved.

Keywords: Supercritical fluid; Titanate coupling reagent; Reaction; Acid–base property; OH groups

1. Introduction

Nanoparticles have many special characteristics and are widely used in the fields of composite materials, biomaterials, sensors, etc., but they have the problem that they are easily agglomerated because of strong interactions between the particles [1]. Good dispersion is the key in many applications. The surfaces of nanoparticles can be modified to give better dispersibility, affinity, functionality, etc. [1–3]. Chemical modification of the particle surface can enhance the dispersibility of nanoparticles in various continuous phases, change the surface activity, and bring about new surface physical and chemical characteristics. For example, nano-SiO₂ particles were used as a DNA carrier after modification by alkoxy silanes and amines that changed the surface potential of the particles [4] and as a fluorescent chemical sensor after modification by organic molecules with fluorescent organic chromophores [5].

Chemical modification of a particle surface can be performed by a reaction between the hydroxyl groups on the surfaces of inorganic oxide particles and modification reagents [4,5]. Fully hydroxylated silica contains 4.6 OH/nm² [6,7], which can be considered a physicochemical constant that is independent of the silica type and structural characteristics, e.g., specific surface area, type of pores, and pore size distribution [8]. There are 12–14 OH/nm² on the (111) surface of a fully hydroxylated titania powder [9]. Infrared spectroscopy [7, 10], thermogravimetric analysis [9,11–13], chemical methods such as titration [6,7,11], X-ray photoelectron spectroscopy [14–16], and nuclear magnetic resonance [12,17] can be used to determine the hydroxyl groups on powders. Many inorganic oxide particles are solid acids and/or bases [18]. XPS is a powerful technique for studying acid–base properties [19]. The surface reactivities (acidic and basic) of several inorganic particles were also readily estimated by in situ Fourier transform infrared (FTIR) measurement of ammonia adsorption [20]. Investigations on high-purity materials have revealed that both Lewis and Brønsted acid sites exist on the particle surfaces [21,22].

* Corresponding author. Fax: +86 10 62772051.

E-mail address: wangtj@mail.tsinghua.edu.cn (T.-J. Wang).

There are many methods of surface chemical modification, e.g., liquid methods [4,5], gaseous methods [23], and mechanochemical methods [24]. Each method has its disadvantages. Liquid methods need the modification reagents to be dissolved in solvents, and there are the problems of solvent recovery, long operational procedures, high costs, and severe pollution. Gaseous methods usually operate at a high temperature in order to get the modification reagents to contact the particle surface in molecular form, and the reactors used are usually fluidized beds, fixed beds, agitating beds, etc. Gaseous methods are suitable for particles of micrometer size that do not easily agglomerate, but it is difficult to achieve uniform modification and to treat exhaust gases that contain modification reagents. Mechanochemical methods comprise mixing and grinding of the particles and modification reagents. The energy consumption is high and there is probable contamination of the product by the grinding medium.

Supercritical CO₂ is a green solvent [25,26] that has the characteristics of a high diffusion coefficient like that of a gas, a high solvating power like that of a liquid, low viscosity, low surface tension, and rapid osmosis into microporous materials [27–31] and has been widely used in material science for its unique properties [30,31]. When supercritical CO₂ is used as the solvent in a surface chemical modification process, the modification reagent can get into the voids of agglomerated particles, so that the modification reagent can contact the particle surface uniformly and react with hydroxyl groups on the surface. A more uniform modification of the particle surface is achieved [32]. Particle modification in supercritical CO₂ does not lead to “caking” of the particles [32] and is especially suitable for nanoparticles. The CO₂ solvent can be separated quickly and outright from the particles by changing the temperature and pressure. There is little or no solvent waste. Tripp and Combes [33] studied the interaction between supercritical CO₂ and a fumed silica with infrared spectroscopy and reported that the physisorption of CO₂ with isolated SiOH groups was weak. Combes et al. [34] studied the chemical modification of a silica wafer surface in supercritical CO₂ with in situ infrared spectroscopy and the utility of CO₂ as a solvent for the reaction of organosilanes with silica was demonstrated with hexamethyldisilazane (HMDS) and octadecyltrichlorosilane (OTS). For HMDS, the byproduct was weakly physisorbed on the hydroxyl groups of the surface and was easily removed by evacuation or purging. Physisorption of OTS from supercritical CO₂ occurred by weak interaction with surface hydroxyl groups. Jia et al. [35] studied the chemical modification of the buried interfaces between silicon wafers and either polystyrene or poly(methyl methacrylate) (PMMA) with the reagent (tridecafluoro-1,1,2,2-tetrahydrooctyl)dimethylchlorosilane (FDCS), using liquid and supercritical CO₂ as the solvent and infusing reagent. Above the critical point of CO₂, FDCS reacted with silanols at the SiO₂/polystyrene interface to form a monolayer. Due to strong hydrogen bonding between PMMA and the silicon substrate, there was only limited modification of the SiO₂/PMMA interface. In our previous research [36,37], the organic modification of ultrafine particles and nanoparticles was performed using CO₂ as the solvent, and it was found that supercritical and liquid

CO₂ are green and effective solvents in the organic modification of inorganic particles.

In this paper, the adsorption and reaction in supercritical CO₂ of the titanate coupling reagent NDZ-201 on the surfaces of seven oxide particles, namely, SiO₂, Al₂O₃, ZrO₂, TiO₂ (anatase), TiO₂ (rutile), Fe₂O₃, and Fe₃O₄, are reported. The influence of the surface properties on the adsorption and reaction was studied by FTIR and TG analysis.

2. Experimental

2.1. Materials

The titanate coupling reagent used, NDZ-201, (CH₃)₂-CHOTi(OP(O)(OH)OP(O)(OC₈H₁₇)₂)₃ [isopropyl tri(diocetylpyrophosphate)titanate] (for short, CA7), was of technical grade (Nanjing Shuguang Chemical Group Co., Ltd., Nanjing, China) with a boiling point of 77 °C and decomposition temperature of 210 °C. The 2-propanol used was of analytical reagent (AR) grade with a purity higher than 99.7% (Beijing Chemical Plant, Beijing, China). The purity of the CO₂ (Beijing Huayuan Gas Corporation, Beijing, China) used was 99.95%. The nanoparticles were commercial products of technical grade; their purities and diameters are listed in Table 1. The two kinds of titania particles in Table 1 had different lattice structures, which were anatase and rutile.

2.2. Determination of OH surface density

The determination of the OH surface density was performed similarly to the procedure described in the literature [9] by TG analysis (TGA2050, TA Instruments, USA). The nanoparticles were heated in nitrogen from room temperature to 120 °C at 10 °C/min, held at this temperature for 10 min (step 1), and then heated at 20 °C/min to 800 °C and held at this temperature for 10 min under nitrogen (step 2). The isothermal hold at 120 and 800 °C is to give better accuracy of the OH density measurement. According to literature reports, physically adsorbed water can be removed at 120 °C in step 1 [8,38,39]. The weight loss in step 2 resulted from the removal of OH groups on the nanoparticle surface [39]. There could be desorption of volatile organic compounds left from particle synthesis or processing, but since it was verified from the FTIR spectra that there were no volatile organic compounds on our particles, the weight loss in step 2 is attributed to the removal of OH groups.

The specific surface areas (SSA) of the nanoparticles were the BET surface areas measured by a surface area analyzer (ASAP2010, Micromeritics Instruments Corp., USA). These are listed in Table 1.

To determine the silanol number density, calibration with different samples containing known amounts of OH groups is necessary [8]. The OH surface density of the nanoparticles was calculated using the TGA weight loss in step 2 and the SSA [9],

$$C_{\text{OH}} = \alpha \times \left[2 \times (W_{120} - W_{800}) \times N_{\text{A}} / (W_{120} \times \text{MW}_{\text{w}} \times \text{SSA} \times 10^{18}) + C_{\text{OH},800} \times W_{800} / W_{120} \right], \quad (1)$$

Table 1
Particle characteristics and experimental results

Particle	SiO ₂	Al ₂ O ₃	ZrO ₂	TiO ₂ (A)	TiO ₂ (R)	Fe ₂ O ₃	Fe ₃ O ₄
Trade No.	A200 ^a	MC2R ^b	HTZr01 ^c	HR3 ^b	DJ3 ^b	HTFe02 ^c	HTFe03 ^c
Purity (%)	≥99.8	≥99.99	≥99.9	≥98.0	≥98.0	–	–
Average diameter (nm)	12	10	20	5	40	50	50
SSA (m ² /g)	233	227	20	282	17	12	19
Added quantity (g)	0.52	1.12	13.93	2.92	6.81	9.24	7.01
CA7/ particle (mol/mol)	0.475	0.375	0.036	0.113	0.048	0.071	0.136
W ₁₂₀ (%)	99.58	95.24	99.83	95.95	99.84	99.73	99.78
W ₈₀₀ (%)	98.37	90.07	99.31	88.12	99.38	97.15	98.62
C _{OH} (OH/nm ²)	2.8	9.9	10.8	12.0	11.3	89.6	25.2
Inflection point temperature (°C)							
Unmodified	–	–	–	–	–	252	284
Nonextracted	232	262	260	220	259	231	265
Extracted	491	284	264	217	308	251	280
W ₀ (%)	98.86	94.09	99.22	90.06	99.56	97.39	98.76
W ₁ (%)				20.41			
W ₂ (%)							
Nonextracted	87.49	84.10	98.45	83.17	98.28	96.71	97.34
Extracted	97.36	87.63	99.03	87.71	–	–	–
W _{CA7} (%)							
Nonextracted	16.85	15.59	0.98	10.91	1.69	0.89	1.84
Extracted	1.94	9.55	0.24	3.47	–	–	–
N _{CA7} (10 ⁻⁷ mol/m ²)							
Nonextracted	5.52	5.24	3.75	2.95	7.59	5.67	7.37
Extracted	0.64	3.21	0.90	0.94	–	–	–

^a Produced by Degussa AG (Germany).

^b Produced by Zhejiang Hongshengrial Material Technology Co., Ltd. (Zhoushan, China).

^c Produced by Nanjing High Technology Nano Co., Ltd. (Nanjing, China).

where C_{OH} is the OH surface density of the nanoparticles, OH/nm², i.e., the number of hydroxyls per unit area; W₁₂₀ is the sample weight at 120 °C, %; W₈₀₀ is the sample weight at 800 °C, %; MW_w is the molecular weight of water, 18 g/mol; N_A is Avogadro's number, 6.022 × 10²³ mol⁻¹; SSA is the specific surface area of particles, m²/g; C_{OH,800} is the OH surface density remaining after 800 °C, OH/nm²; and α is a calibration factor.

2.3. Sample preparation and analysis

Most of the experimental apparatus and procedures have been described in our previous research [37]. For the simultaneous addition of the various nanoparticles listed in Table 1, seven cubic pillar-shaped baskets made from a 300 mesh (the hole size is about 50 μm) sieve, with length 20 mm, width 8 mm, and height 90 mm, were used to load the nanoparticles. The nanoparticles were usually loose agglomerations that were stable. There was no loss of particles from the mesh baskets in the experiments.

The quantities of added nanoparticles are listed in Table 1. The different particles have almost the same volumes in the baskets. The quantity of added CA7 was 5.4 g. The mole ratios of CA7 to nanoparticles are listed in Table 1. The experimental temperature and pressure were 60 °C and 20.0 MPa. The samples were kept for 1 h at the set conditions, which was sufficient for phase equilibrium and reaction in an agitated state [40,41].

After reaction, the modified particles were extracted with 2-propanol for 72 h and then dried at 120 °C for 24 h to remove

weakly physisorbed CA7 on the surfaces of nanoparticles. In our previous research [37], it was confirmed that an extraction time of 72 h was enough to completely remove CA7 weakly physisorbed on the nanoparticle surfaces.

A Fourier transform IR spectrometer (NICOLET 5DX, USA) was used for IR absorption spectroscopy. The resolution was 2 cm⁻¹, the number of repetitions was 200, and the spectral range was from 4000 to 400 cm⁻¹. KBr was used as the background.

Thermogravimetric analysis (TGA2050, TA Instruments, USA) was also used to determine the quantity of CA7 adsorbed and reacted on the particle surfaces. The samples were heated from room temperature to 800 °C in nitrogen at a heating rate of 20 °C/min. For a more accurate determination, the terminal temperature of 800 °C is higher than that of our previous research [36,37]. The quantity of CA7 on the particle surfaces can be estimated from the weights of the samples at 800 °C by the method given in the references [36,37],

$$W_{CA7} = (W_0 - W_2)/(W_2 - W_1) \times 100\%, \quad (2)$$

$$N_{CA7} = W_{CA7}/(MW_{CA7} \times SSA), \quad (3)$$

where W_{CA7} is the quantity of CA7 on the particle surface, %; W₀ is the weight of unmodified particles at 800 °C, %; W₁ is the weight of CA7 at 800 °C; W₂ is the weight of modified particles at 800 °C, %; N_{CA7} is the quantity of CA7 on the particle surface, mol/m²; SSA is the specific surface area of particles, m²/g; and MW_{CA7} is the molecular weight of CA7, 1311 g/mol.

3. Results and discussion

3.1. OH surface density

The determination of the OH surface density has to be calibrated with different samples containing known amounts of OH groups. The TG curve of SiO₂ (A200) is shown in Fig. 1. For SiO₂, 1 OH/nm² still remains on the surface at 800 °C [42], and without calibration, the OH surface density of SiO₂ (A200) calculated from Eq. (1) is 4.51 OH/nm². Since the OH surface density of SiO₂ (A200) is known to be 2.8 OH/nm² [9], a calibration factor of $\alpha = 0.621$ is used to calculate the OH surface density for the nanoparticles of SiO₂ in Eq. (1). This is very close to the value of 0.625 reported in the literature [9]. The calibration factor α should be obtained for the other nanoparti-

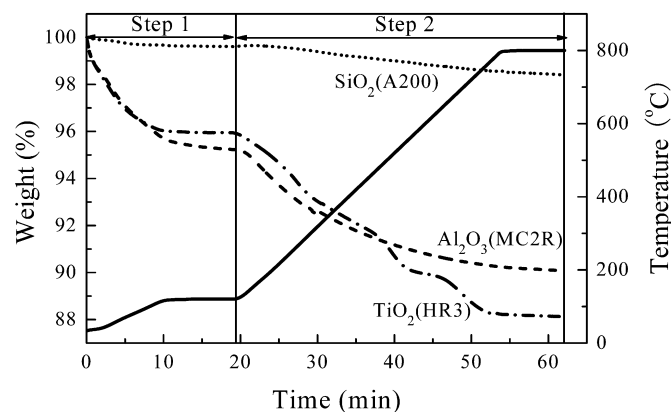


Fig. 1. Weight of pure SiO₂ (A200) particle (dotted line), Al₂O₃ (MC2R) particle (dashed line), TiO₂ (HR3) particle (dotted-dashed line), and TGA temperature (solid line) as a function of TGA heating time.

cles as well, but it is taken as 0.621 for all the nanoparticles in this research.

TiO₂ particles can be considered to be free of OH surface groups at 500 °C [9], but there was still weight loss from the TiO₂ particles in our TG analysis at higher than 500 °C, as shown in Fig. 1. In comparing the OH surface density, 800 °C was taken as the terminal temperature of all the nanoparticles in this research.

To exactly determine the OH surface density, the residual OH surface density at 800 °C has to be known, but this is not known except for SiO₂. Also, the residual OH surface density at 800 °C may vary with the kind of nanoparticles. In this work, it is assumed that the surfaces of all particles other than SiO₂ are free of OH surface groups at 800 °C. The OH surface density of each kind of nanoparticle, measured using TG analysis and estimated from Eq. (1), is listed in Table 1.

3.2. IR analysis

The IR spectra of CA7, unmodified and nonextracted and extracted modified nanoparticles of Al₂O₃, TiO₂ (A), and TiO₂ (R), are shown in Figs. 2–4. The spectra of all nonextracted modified samples showed characteristic absorption peaks at 2961, 2933, 2874, and 2862 cm⁻¹, which are the absorption peaks of the CH₃- and CH₂- groups of the coupling reagent CA7. This indicated that there are CA7 on the particle surfaces. The spectra of extracted modified SiO₂, Al₂O₃, ZrO₂, and TiO₂ (A) particles still showed the absorption peaks of the CH₃- and CH₂- groups. These are shown by the spectra of Al₂O₃ in Fig. 2 and TiO₂ (A) in Fig. 3. However, the spectra of extracted modified TiO₂ (R), Fe₂O₃, and Fe₃O₄ particles did not show the absorption peaks anymore. This is shown by the spectrum of TiO₂ (R) in Fig. 4. It can be inferred that

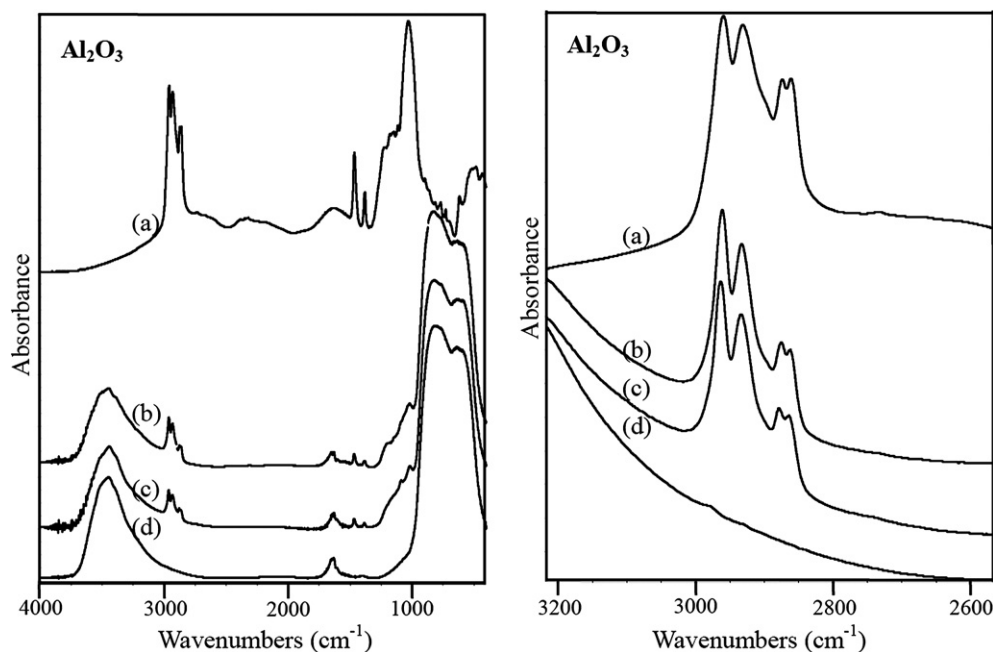


Fig. 2. IR absorption spectra of (a) CA7, (b) Al₂O₃-CA7 (nonextracted), (c) Al₂O₃-CA7 (extracted), and (d) Al₂O₃. The curves on the right have expanded axes.

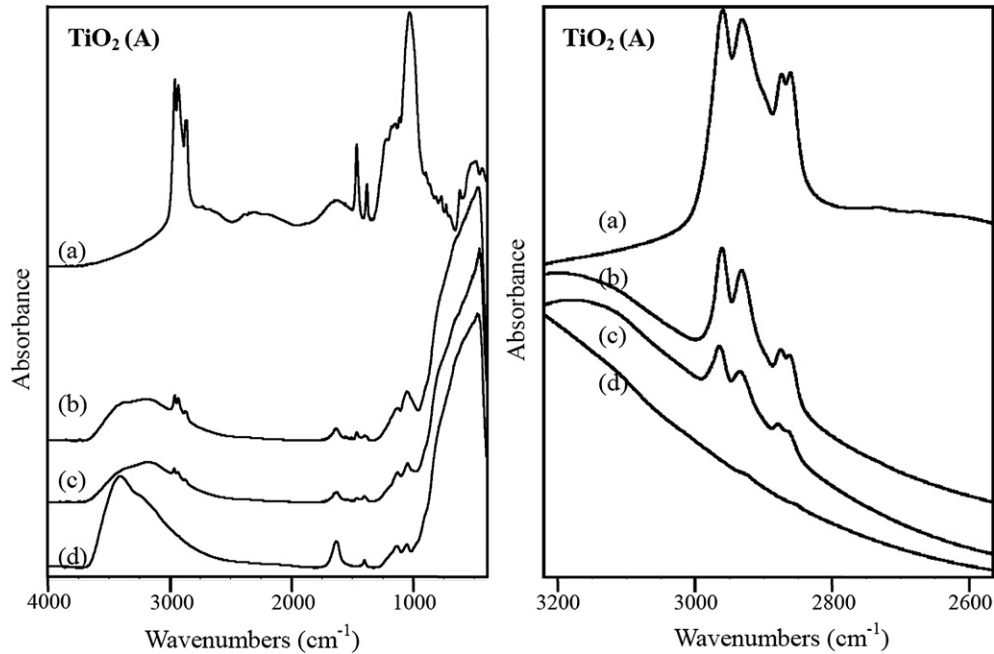


Fig. 3. IR absorption spectra of (a) CA7, (b) TiO₂ (A)-CA7 (nonextracted), (c) TiO₂ (A)-CA7 (extracted), and (d) TiO₂ (A). The curves on the right have expanded axes.

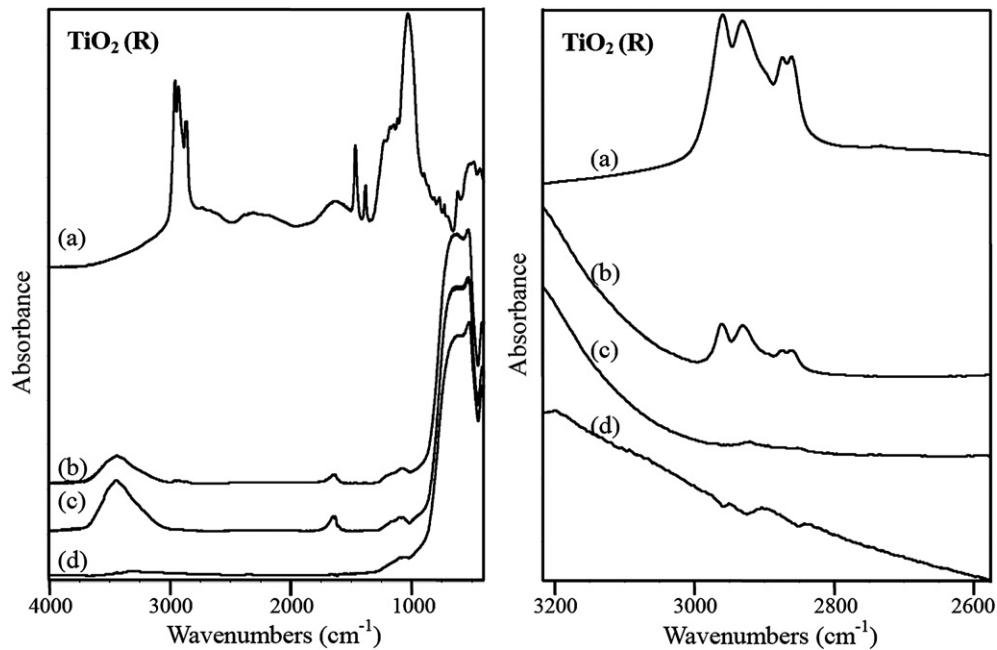


Fig. 4. IR absorption spectra of (a) CA7, (b) TiO₂ (R)-CA7 (nonextracted), (c) TiO₂ (R)-CA7 (extracted), and (d) TiO₂ (R). The curves on the right have expanded axes.

there is only weak adsorption of CA7 on the surfaces of the TiO₂ (R), Fe₂O₃, and Fe₃O₄ particles. Weakly adsorbed CA7 was removed completely from the surfaces of the particles by extraction, and so the spectra of extracted modified TiO₂ (R), Fe₂O₃, and Fe₃O₄ particles did not show absorption peaks of CA7. For the SiO₂, Al₂O₃, ZrO₂, and TiO₂ (A) particles, there was not only weak adsorption of CA7, but also other states of CA7 that were not removed from the surfaces by extraction, as shown by the spectra of extracted modified SiO₂, Al₂O₃,

ZrO₂, and TiO₂ (A) particles still showing the absorption peaks of CA7.

3.3. Thermogravimetric analysis

The organic titanate coupling reagent thermally decomposes at high temperatures in a nitrogen atmosphere. The TG curve of CA7 is shown in Fig. 5a. There is an inflection point at 229 °C where the sample weight sharply decreases. A second weak in-

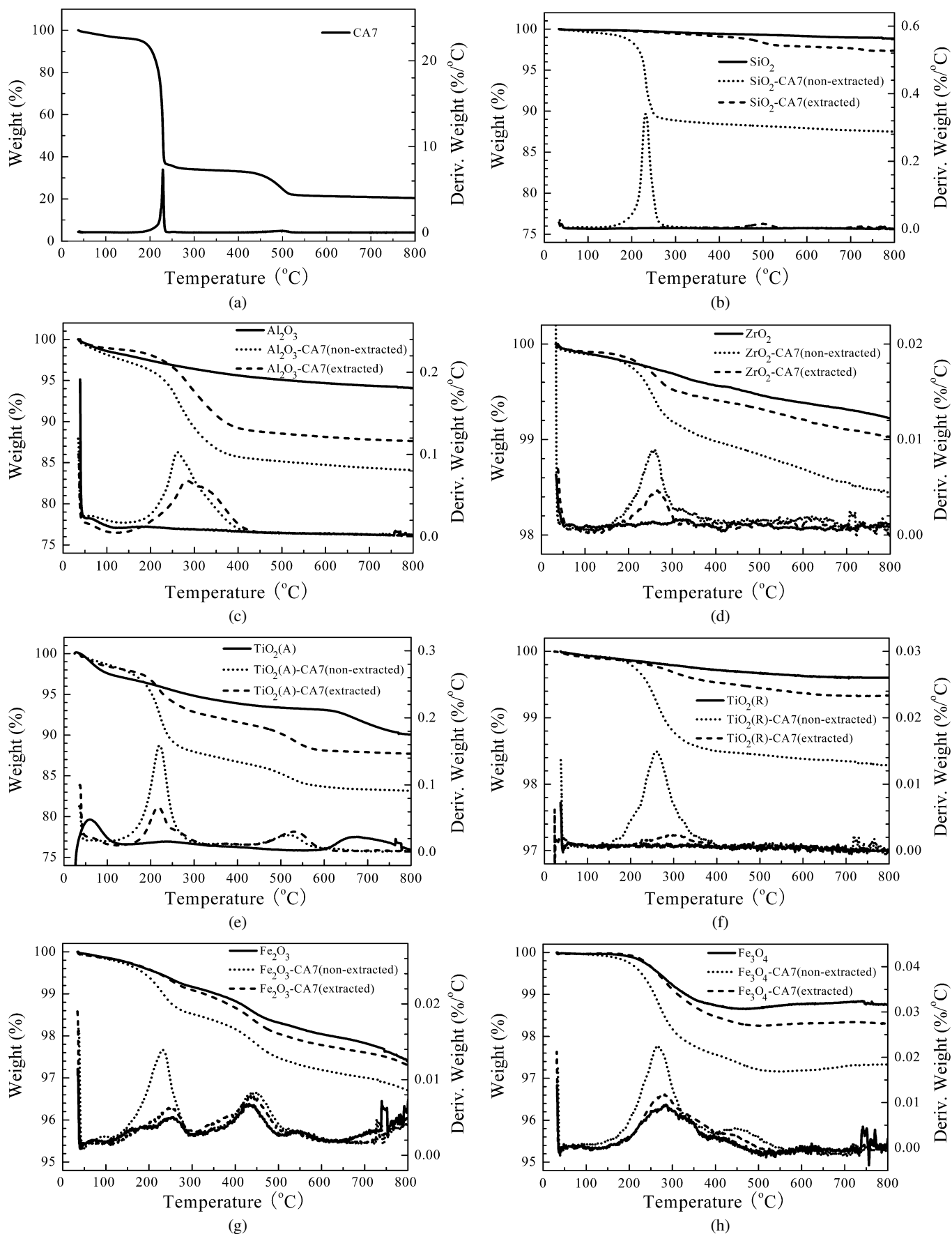


Fig. 5. Weight (upper curves) and deriv. weight (lower curves) of the samples as a function of TGA heating temperature.

flexion point at about 498 °C may correspond to the further decomposition of CA7. Thereafter, the weight of CA7 does not decrease and the remaining weight is 20.41 at 800 °C.

The spectra of the unmodified nanoparticles, and nonextracted and extracted modified nanoparticles are shown in Fig. 5. It can be seen in Fig. 5 that the weights of the unmodified particles decreased as the temperature increased and finally became constant at 800 °C. The weight loss resulted from the desorption of physically adsorbed water and the dehydration of the surface hydroxyl groups. For the modified particles, with CA7 on the surfaces, the weight loss comprised the desorption of physically adsorbed water, dehydration of surface hydroxyl groups, and decomposition of CA7.

There was an inflection point on the TG curves of the nonextracted modified particles. When the temperature was lower than the inflection point temperature, the weight decreased slowly, similarly to the behavior of unmodified particles. When the temperature was near the inflection point, the weight decreased rapidly. When the temperature was higher than the inflection point temperature, the weight decreased slowly again and became constant at about 800 °C. The inflection point temperatures of all the nonextracted modified particles are listed in Table 1.

For SiO₂, Al₂O₃, ZrO₂, TiO₂ (A), it is shown in Figs. 5b–5e that the weight loss from the extracted modified particles was clearly lower than that from the nonextracted modified particles, since weakly adsorbed CA7 was removed from the particle surfaces by extraction with 2-propanol. As there was CA7 remaining on the surfaces, the weight loss from the extracted modified particles was higher than that from the unmodified particles and also became constant at about 800 °C. As with the nonextracted modified particles, there was also an inflection point temperature on the TG curves of the extracted modified particles. In the case of SiO₂, it is shown in Fig. 5b that the inflection point temperature of the extracted modified particles was 491 °C, which is much higher than that of the nonextracted modified particles, which was 231 °C. This showed that there was a chemical reaction of CA7 on SiO₂ surface. For Al₂O₃, it is shown in Fig. 5c that the inflection point temperature of the extracted modified particles was 284 °C, which is higher than that of the nonextracted modified particles, which was 262 °C. This also showed that there was a chemical reaction of CA7 on Al₂O₃ surface. For ZrO₂ and TiO₂ (A), it is shown in Figs. 5d and 5e that the inflection point temperature of the extracted modified particles was almost the same as that of the nonextracted modified particles. This indicated that there was no surface chemical reaction of CA7. Thus, there was a chemical reaction of CA7 on the surfaces of SiO₂ and Al₂O₃, and only strong adsorption on the surfaces of ZrO₂ and TiO₂ (A).

For TiO₂ (R), Fe₂O₃, and Fe₃O₄, from the FTIR analysis, there was no CA7 on the surfaces after extraction, but the weight loss from the extracted modified particles was a little higher than that from the unmodified particles, as shown in Figs. 5f–5h. The difference in the weight loss between the extracted modified particles and the unmodified particles may be due to experimental uncertainties in the sample preparation and TGA measurement. There was also an inflection point on the

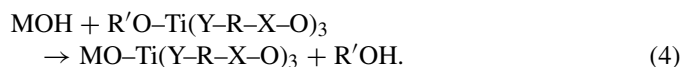
TG curves of the extracted modified particles. In the cases of the Fe₂O₃ and Fe₃O₄ particles, it is shown in Figs. 5g and 5h that the inflection point temperature of the extracted modified particles was the same as that of the unmodified particles. For TiO₂ (R), it is shown in Fig. 5f that the inflection point temperature of the extracted modified particles was higher than that of the nonextracted modified particles, and there was no inflection point temperature with the unmodified particles, and so the difference in the inflection point temperature between the extracted modified particles and nonextracted modified particles may be due to experimental uncertainties in the sample preparation and TGA measurement.

From the above experimental results and analysis, it is concluded that the states of CA7 on different particle surfaces were different: for SiO₂ and Al₂O₃, there were adsorption and also chemical bonding, for ZrO₂ and TiO₂ (A), there were both weak and strong adsorption, and for Fe₂O₃, Fe₃O₄, and TiO₂ (R), there was only weak adsorption.

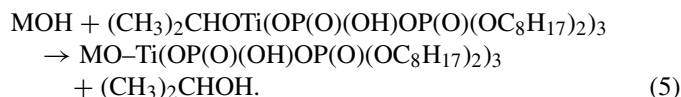
From Eqs. (2) and (3), the quantities of CA7 on the particle surfaces can be estimated from the TG data at 800 °C. The results are listed in Table 1.

3.4. Surface reaction mechanism

The chemical reaction mechanism of the titanate coupling reagents on the inorganic surfaces is the following [43–45]:



For CA7, Eq. (4) is written as



There are one isopropoxy and three organic long chains in the structural formula of CA7. The isopropoxy group can react with protons on the particle surfaces to form 2-propanol and the remaining group forms a chemical bond on the particle surface. The protons come from the hydroxyl groups on the particle surfaces.

The reaction of CA7 depends on the surface characteristics of the particles. It can be seen from Eqs. (4) and (5) that protons provided by the particle surfaces are the key for the reaction to occur.

Although there are plenty of OH groups on nanoparticle surfaces, the characteristics of the OH groups for different particles are different. The acidity or basicity of the OH groups on the particle surfaces determines whether the surface chemical reaction of the titanate coupling reagent occurs. For SiO₂ and Al₂O₃ particles, it is deduced that the OH groups on their surfaces can provide protons to react with CA7. For ZrO₂, TiO₂ (A), TiO₂ (R), Fe₂O₃, and Fe₃O₄ particles, there are no protons on the surfaces that can react with CA7. A chemical reaction of titanate coupling reagents on these particle surfaces can be induced by surface pretreating, such as by precoating with SiO₂ and Al₂O₃ films [36].

Since the reaction environments are the same, that is, the same solvent (supercritical CO₂), concentration of CA7, volume of particles, reaction time (1 h), extraction solvent (2-propanol), time (72 h), etc., the average reactivity of the surface OH groups with CA7 can be defined as

$$R_{OH} = (N_{CA7,r} \times N_A) / (C_{OH} \times 10^{18}), \quad (6)$$

where R_{OH} is the average reactivity of the surface OH groups with CA7 and $N_{CA7,r}$ is the quantity of CA7 chemically reacted on the particle surface, mol/m².

From Eq. (6), R_{OH} of SiO₂ and Al₂O₃ are calculated to be 0.014 and 0.020, respectively. This shows that the average reactivity of the surface OH groups of Al₂O₃ particles with CA7 is higher than that of SiO₂ particles.

4. Conclusion

The adsorption and reaction of the titanate coupling reagent NDZ-201 on different particle surfaces in supercritical CO₂ are different. On SiO₂ and Al₂O₃ particles, there is a chemical reaction of the titanate coupling reagent on the surfaces; on the surfaces of ZrO₂ and TiO₂ (A) particles, there are weak and strong adsorption of the titanate coupling reagent; and on TiO₂ (R), Fe₂O₃, and Fe₃O₄ particles, there is only weak adsorption. The acidity or basicity of the OH groups on a particle surface determines whether a chemical reaction with the titanate coupling reagent occurs on the particle surfaces. SiO₂ and Al₂O₃ particles have OH groups on their surfaces that can provide protons to react with the titanate coupling reagent. ZrO₂, TiO₂ (A), TiO₂ (R), Fe₂O₃, and Fe₃O₄ particles do not provide protons to react with the titanate coupling reagent. A chemical reaction of the titanate coupling reagent with these particle surfaces can be brought about by a prior modification of the surface acid–base property. The reactivity of the surface OH groups with the titanate coupling reagent is higher on Al₂O₃ than on SiO₂ particles.

Acknowledgments

The authors wish to express their appreciation of the financial support of this study by the National Natural Science Foundation of China (NSFC No. 20476051) and the Special Research Fund for the Doctoral Program of Higher Education (China) (SRFDP No. 200330003044).

References

- [1] G.Y. Tolnai, F. Csempesz, M. Kabai-Faix, E. Kalman, Z. Keresztes, A.L. Kovacs, J.J. Ramsden, Z. Horvolgyi, *Langmuir* 17 (2001) 2683.
- [2] Q.F. Liu, D.A. Spears, Q.P. Liu, *Appl. Clay Sci.* 19 (2001) 89.
- [3] Y.L. Lin, T.J. Wang, C. Qing, J. Yang, Y. Jin, *Chem. J. Chin. Univ.-Chin.* 22 (2001) 104, in Chinese.
- [4] Z. Csogor, M. Nacken, M. Sameti, C.M. Lehr, H. Schmidt, *Mater. Sci. Eng. C Biomimet. Supramol. Syst.* 23 (2003) 93.
- [5] H. Wang, X.H. Zhang, S.K. Wu, *Acta Chim. Sin.* 61 (2003) 1921, in Chinese.
- [6] C.G. Armistead, A.J. Tyler, F.H. Hambleton, S.A. Mitchell, J.A. Hockey, *J. Phys. Chem.* 73 (1969) 3947.
- [7] J.J. Fripiat, J.J. Uytterhoeven, *J. Phys. Chem.* 66 (1965) 800.
- [8] E.F. Vansant, P. Van Der Voort, K.C. Vrancken, *Characterization and Chemical Modification of the Silica Surface*, Elsevier, Amsterdam, 1995.
- [9] R. Mueller, H.K. Kammler, K. Wegner, S.E. Pratsinis, *Langmuir* 19 (2003) 160.
- [10] M.A. Ramos, M.H. Gil, E. Schacht, G. Matthys, W. Mondelaers, M.M. Figueiredo, *Powder Technol.* 99 (1998) 79.
- [11] G.E. Kellum, R.C. Smith, *Anal. Chem.* 39 (1967) 341.
- [12] R.K. Gilpin, M.E. Gangoda, M. Jaroniec, *Carbon* 35 (1997) 133.
- [13] T.M.H. Costa, M.R. Gallas, E.V. Benvenuti, J.A.H. daJornada, *J. Non-Cryst. Solids* 220 (1997) 195.
- [14] G.W. Simmons, B.C. Beard, *J. Phys. Chem.* 91 (1987) 1143.
- [15] E. McCafferty, J.P. Wightman, *Surf. Interface Anal.* 26 (1998) 549.
- [16] B. Erdem, R.A. Hunsicker, G.W. Simmons, E.D. Sudol, V.L. Dimonie, M.S. El-Aasser, *Langmuir* 17 (2001) 2664.
- [17] V.M. Bermudez, *J. Phys. Chem.* 74 (1970) 4160.
- [18] K. Tanabe, M. Misono, Y. Ono, H. Hattori, *New Solid Acids and Bases*, Elsevier, Amsterdam, 1989.
- [19] W.M. Mullins, B.L. Averbach, *Surf. Sci.* 206 (1988) 29.
- [20] M. Primet, P. Pichat, M.V. Mathieu, *J. Phys. Chem.* 75 (1971) 1221.
- [21] G. Busca, H. Saussey, O. Saur, J.C. Lavalley, V. Lorenzelli, *Appl. Catal.* 14 (1985) 245.
- [22] T. Bezrodna, G. Puchkovska, V. Shimanovska, I. Chashechnikova, T. Khalyavka, J. Baran, *Appl. Surf. Sci.* 214 (2003) 222.
- [23] Y.E. Kim, S.G. Kim, H.J. Shin, S.Y. Ko, S.H. Lee, *Powder Technol.* 139 (2004) 81.
- [24] W. Wu, S.C. Lu, *Powder Technol.* 137 (2003) 41.
- [25] M. Poliakov, M.W. George, S.M. Howdle, V.N. Bagratashvili, B.X. Han, H.K. Yan, *Chin. J. Chem.* 17 (1999) 212.
- [26] W. Leitner, *Accounts Chem. Res.* 35 (2002) 746.
- [27] Z.H. Wang, J.H. Dong, N.P. Xu, J. Shi, *AIChE J.* 43 (1997) 2359.
- [28] P. Subra, P. Jestin, *Powder Technol.* 103 (1999) 2.
- [29] J.M. Blackburn, D.P. Long, A. Cabanas, J.J. Watkins, *Science* 294 (2001) 141.
- [30] A.I. Cooper, *Adv. Mater.* 15 (2003) 1049.
- [31] F. Cansell, C. Aymonier, A. Loppinet-Serani, *Curr. Opin. Solid State Mater. Sci.* 7 (2003) 331.
- [32] J.R. Combes, H.K. Mahabadi, C.P. Tripp, *Patent US 5,725,987*, 1998.
- [33] C.P. Tripp, J.R. Combes, *Langmuir* 14 (1998) 7348.
- [34] J.R. Combes, L.D. White, C.P. Tripp, *Langmuir* 15 (1999) 7870.
- [35] X.Q. Jia, T.J. McCarthy, *Langmuir* 18 (2002) 683.
- [36] Z.W. Wang, T.J. Wang, Z.W. Wang, Y. Jin, *Powder Technol.* 139 (2004) 148.
- [37] Z.W. Wang, T.J. Wang, Z.W. Wang, Y. Jin, *J. Supercrit. Fluids* 37 (2006) 125.
- [38] J.A. Hockey, *Chem. Ind.* 9 (1965) 57.
- [39] R.K. Iler, *The Chemistry of Silica*, Wiley, New York, 1979.
- [40] A.J. Jay, D.C. Steytler, *J. Supercrit. Fluids* 5 (1992) 274.
- [41] D. Tuma, G.M. Schneider, *Fluid Phase Equilib.* 158–160 (1999) 743.
- [42] G. Curthoys, V.Y. Davydov, A.V. Kiselev, S.A. Kiselev, B.V. Kuznetsov, *J. Colloid Interface Sci.* 48 (1974) 58.
- [43] S.J. Monte, G. Sugeran, *Polym. Eng. Sci.* 24 (1984) 1369.
- [44] M. Hussain, A. Nakahira, S. Nishijima, K. Niihara, *Mater. Lett.* 26 (1996) 299.
- [45] J. Gonzalez, C. Albano, M. Ichazo, M. Hernandez, R. Sciamanna, *Polym. Degrad. Stab.* 73 (2001) 211.